Electronic Supplementary Information for

Trimetallic PdCuIr with long-spined sea-urchin-like morphology for ambient electroreduction of nitrogen to ammonia

Rajaiah Dhilip Kumar,‡ Ziqiang Wang,‡ Chunjie Li, Alam Venugopal Narendra Kumar, Hairong Xue, You Xu, Xiaonian Li, Liang Wang* and Hongjing Wang*

State Key Laboratory Breeding Base of Green-Chemical Synthesis Technology, College of Chemical Engineering, Zhejiang University of Technology, Hangzhou 310014, P. R. China.

*Corresponding authors' E-mails: wangliang@zjut.edu.cn; hjw@zjut.edu.cn.

‡ Rajaiah Dhilip Kumar and Ziqiang Wang have made equal contribution to this paper.

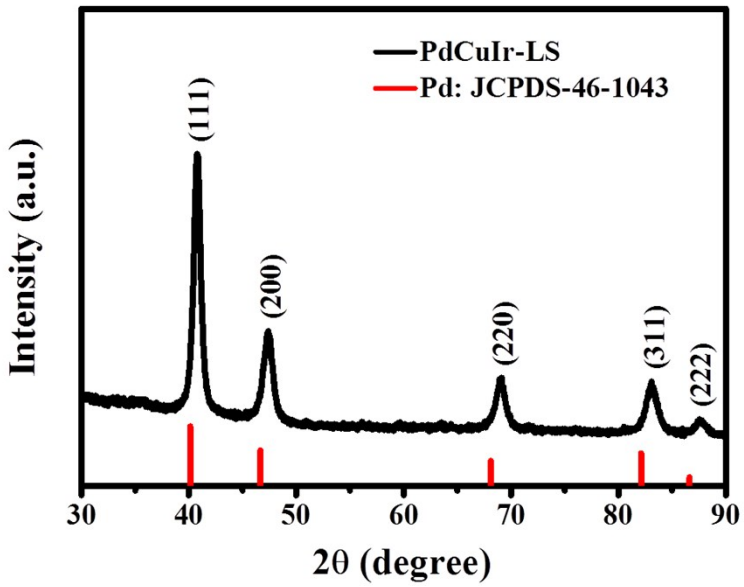

Fig. S1 XRD pattern of the PdCuIr-LS.

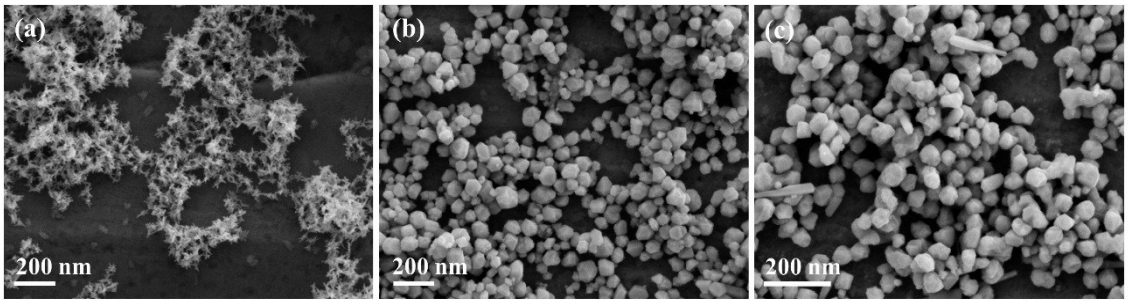

Fig. S2 SEM images of the samples prepared with different precursors under the identical conditions: (a) PdCu, (b) PdIr and (c) Pd nanoparticles.

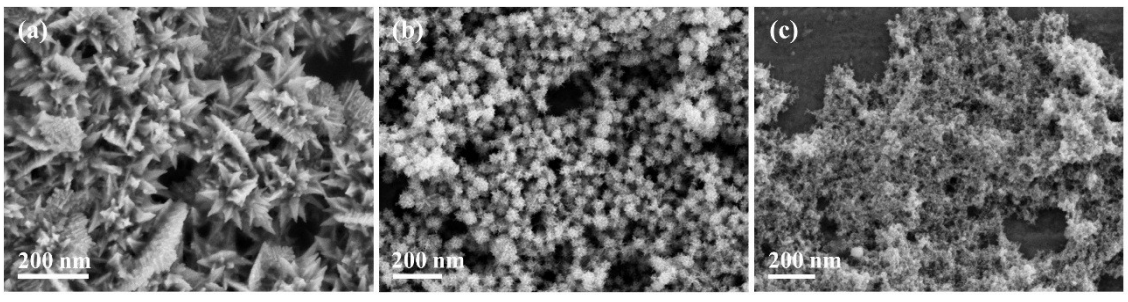

Fig. S3 SEM images of the samples prepared without (a) F127, (b) KBr and (c) HCl under the identical conditions.

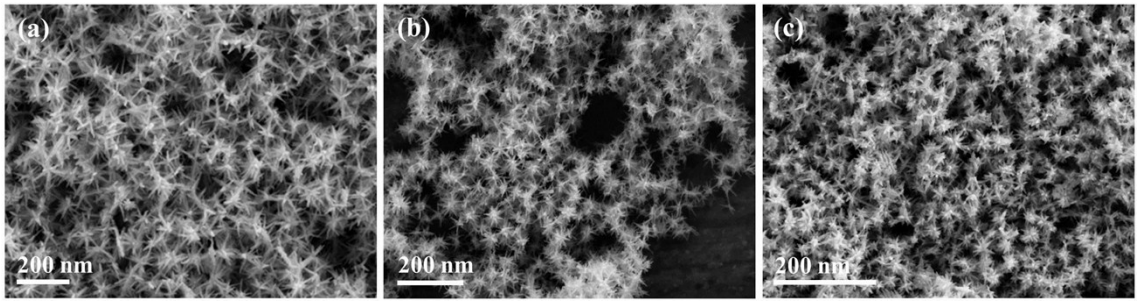

Fig. S4 SEM images of the PdCuIr samples prepared with different amounts of metallic precursors under the identical conditions: (a) Na_2PdCl_4 (2.5 mL, 20 mM), $CuCl_2$ (1.0 mL, 20 mM), $IrCl_3$ (1.0 mL, 20 mM); (b) Na_2PdCl_4 (1.5 mL, 20 mM), $CuCl_2$ (1.5 mL, 20 mM), $IrCl_3$ (1.5 mL, 20 mM); (c) Na_2PdCl_4 (3.0 mL, 20 mM), $CuCl_2$ (0.75 mL, 20 mM), $IrCl_3$ (0.75 mL, 20 mM).

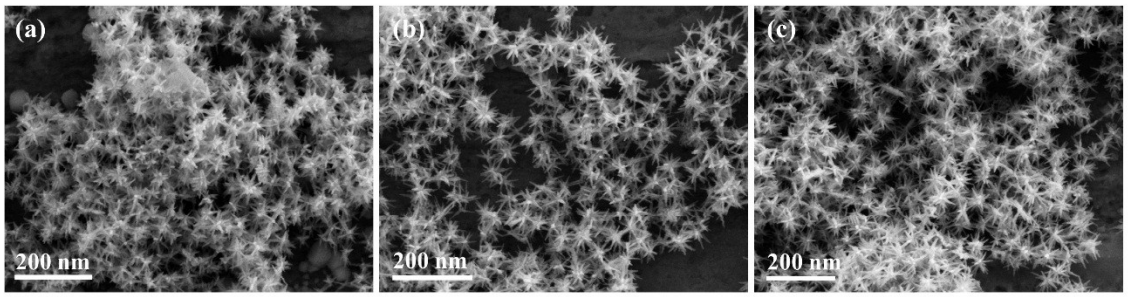

Fig. S5 SEM images of the PdCuIr alloys prepared at different reaction times: (a) 15 min, (b) 60 min and (c) 90 min.

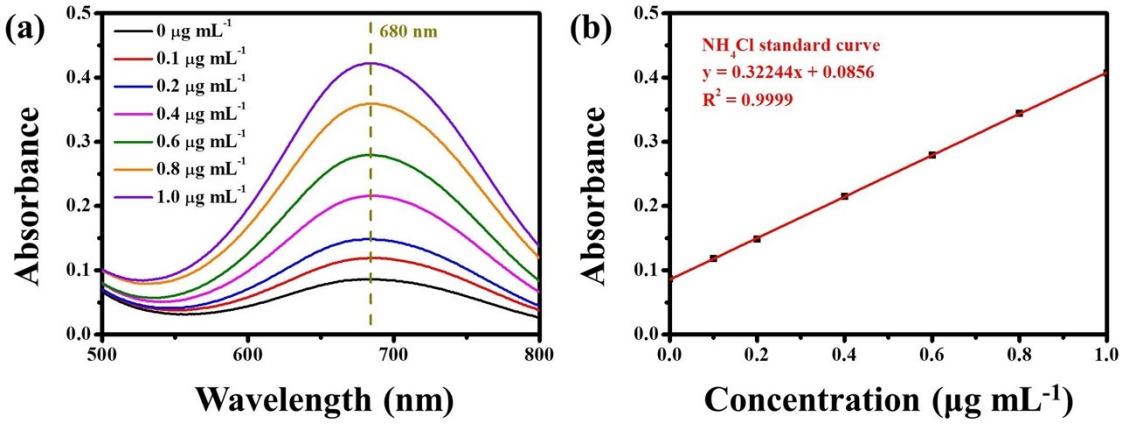

Fig. S6 (a) UV-vis absorption spectra of standard NH_4Cl solution colored with indophenol assays for 2 h at room temperature. (b) The linear relationship between maximum absorbance at λ = 680 nm and concentrations of NH_4Cl solution (y = 0.32244x + 0.0856, R^2 = 0.9999).

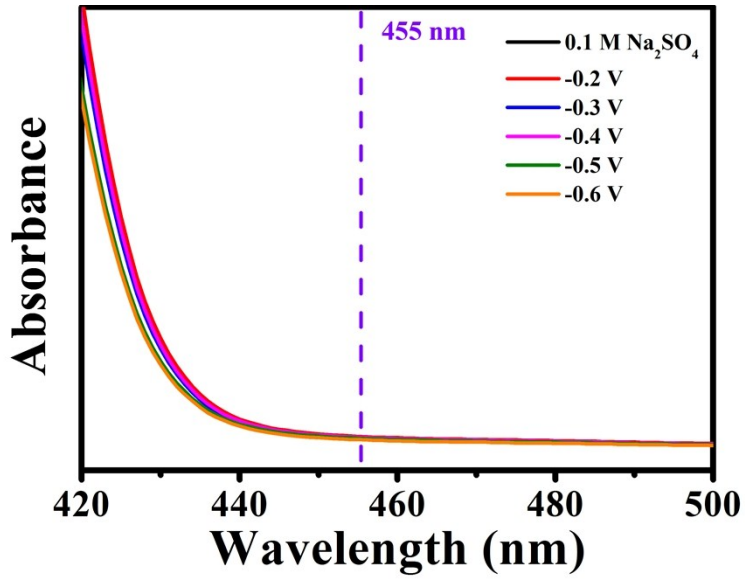

Fig. S7 UV-vis absorption spectra of different electrolytes mixed with N_2H_4 color reagent for 20 min at room temperature. The absorbance was determined at a wavelength of 455 nm.

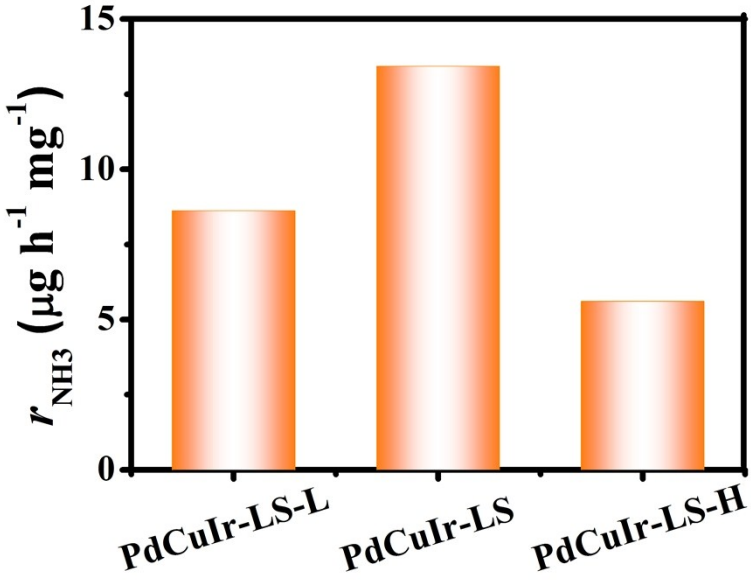

Fig. S8 Average NH_3 yield of different samples at –0.3 V.

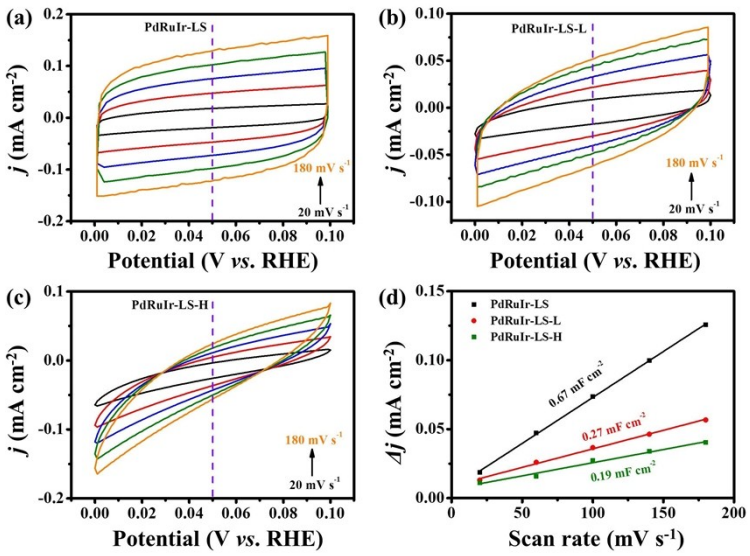

Fig. S9 (a-c) Cyclic voltammetry curves of different samples at various scan rates in the potential range between 0 and 0.1 V. (d) Current density differences at 0.05 V plotted against scan rates.

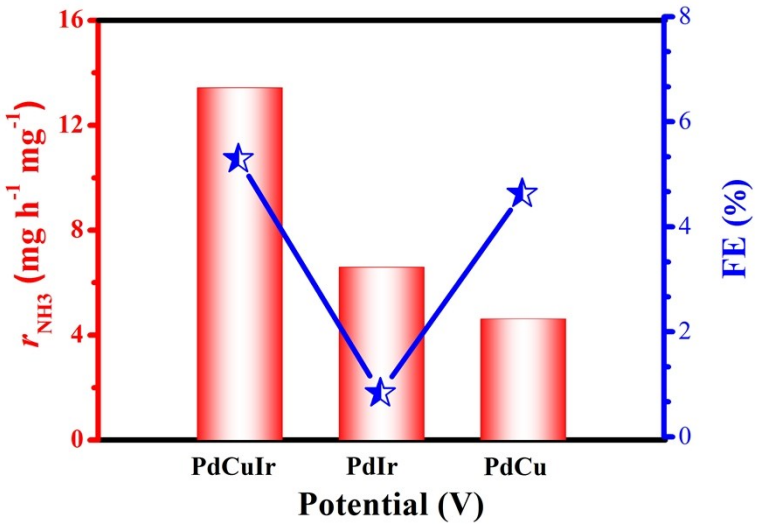

Fig. S10 Average NH_3 yield and Faradaic efficiency for the different samples at –0.3 V.

Table S1. Comparison of the NRR performance of the PdCuIr-LS with recently reported electrocatalysts under ambient conditions.

Electrocatalysts	Electrolytes	r_{NH3}	FE	Ref.
PdCuIr-LS	**0.1 M Na_2SO_4**	**13.43 μg h^{-1} mg^{-1} (8.7×10^{-11} mol s^{-1} cm^{-2})**	**5.29%**	**This work**
MoO_3	0.1 M HCl	29.43 μg h^{-1} mg^{-1}	1.9%	1
Rh nanosheet	0.1 M KOH	23.9 μg h^{-1} mg^{-1}	0.22%	2
N-doped porous carbon	0.05 M H_2SO_4	23.8 μg h^{-1} mg^{-1}	1.42%	3
TiO_2-rGO	0.1 M Na_2SO_4	15.13 μg h^{-1} mg^{-1}	3.3%	4
α-Au/CeO_x-rGO	0.1 M HCl	8.31 μg h^{-1} mg^{-1}	10.1%	5
Au nanorods	0.1 M KOH	6.04 μg h^{-1} mg^{-1}	4%	6
VN nanosheet array	0.1 M HCl	5.6 μg h^{-1} $mg^{-1}_{cat.}$	2.25%	7
Pd/C	0.1 M HCl	~2.5 μg h^{-1} $mg^{-1}_{cat.}$	~1.0%	8
$Pd_{0.2}Cu_{0.8}$/rGO	0.1 M KOH	2.80 μg h^{-1} mg^{-1}	~0.71%	9
γ-Fe_2O_3	0.1 M KOH	0.21 μg h^{-1} mg^{-1}	1.9%	10
MoS_2/CC	0.1 M Na_2SO_4	8.08×10^{-11} mol s^{-1} cm^{-2}	1.17	11
Fe_3O_4/Ti	0.1 M Na_2SO_4	5.6×10^{-11} mol s^{-1} cm^{-2}	2.6	12
PEBCD/C	0.5 M Li_2SO_4	2.58×10^{-11} mol s^{-1} cm^{-2}	2.85	13
Fe_2O_3-CNT	$KHCO_3$	0.36×10^{-11} mol s^{-1} cm^{-2}	0.15	14
Ru/C	2 M KOH	0.34×10^{-11} mol s^{-1} cm^{-2}	0.28	15

Table S2. The compositions of samples prepared with different metal precursors.

Samples	Mole ratios
PdCuIr-LS	10/4/1
PdCuIr-LS-L	5/5/1
PdCuIr-LS-H	12/3/1

References

1 J. Han, X. Ji, X. Ren, G. Cui, L. Li, F. Xie, H. Wang, B. Li and X. Sun, *J. Mater. Chem. A*, 2018, **6**, 12974–12977.

2 H.-M. Liu, S.-H. Han, Y. Zhao, Y.-Y. Zhu, X.-L. Tian, J.-H. Zeng, J.-X. Jiang, B. Y. Xia and Y. Chen, *J. Mater. Chem. A*, 2018, **6**, 3211–3217.

3 Y. Liu, Y. Su, X. Quan, X. Fan, S. Chen, H. Yu, H. Zhao, Y. Zhang and J. Zhao, *ACS Catal.*, 2018, **8**, 1186–1191.

4 X. Zhang, Q. Liu, X. Shi, A. M. Asiri, Y. Luo, X. Sun and T. Li, *J. Mater. Chem. A*, 2018, **6**, 17303–17306.

5 S.-J. Li, D. Bao, M.-M. Shi, B.-R. Wulan, J.-M. Yan and Q. Jiang, *Adv. Mater.*, 2017, **29**, 1700001.

6 D. Bao, Q. Zhang, F. L. Meng, H. X. Zhong, M. M. Shi, Y. Zhang, J. M. Yan, Q. Jiang and X. B. Zhang, *Adv. Mater.*, 2017, **29**, 1604799.

7 R. Zhang, Y. Zhang, X. Ren, G. Cuo, A. M. Asiri, B. Zheng and X. Sun, *ACS Sustainable Chem. Eng.*, 2018, **6**, 9545–9549.

8 J. Wang, L. Yu, L. Hu, G. Chen, H. Xin and X. Feng, *Nat. Commun.*, 2018, **9**, 1795.

9 M.-M. Shi, D. Bao, S.-J. Li, B.-R. Wulan, J.-M. Yan and Q. Jiang, *Adv. Energy Mater.*, 2018, **8**, 1800124.

10 J. Kong, A. Lim, C. Yoon, J. H. Jang, H. C. Ham, J. Han, S. Nam, D. Kim, Y.-E. Sung, J. Choi and H. S. Park, *ACS Sustainable Chem. Eng.*, 2017, **5**, 10986–10995.

11 L. Zhang, X. Ji, X. Ren, Y. Ma, X. Shi, Z. Tian, A. M. Asiri, L. Chen, B. Tang and X. Sun, *Adv. Mater.*, 2018, **30**. 1800191.

12 Q. Liu, X. Zhang, B. Zhang, Y. Luo, G. Cui, F. Xie and X. Sun, *Nanoscale*, 2018, **10**, 14386–14389.

13 G. F. Chen, X. Cao, S. Wu, X. Zeng, L. X. Ding, M. Zhu and H. Wang, *J. Am. Chem. Soc.*, 2017, **139**, 9771–9774.

14 S. Chen, S. Perathoner, C. Ampelli, C. Mebrahtu, D. Su and G. Centi, *Angew. Chem., Int. Ed.*, 2017, **56**, 2699–2703.

15 V. Kordali, G. Kyriacou and C. Lambrou, *Chem. Commun.*, 2000, 1673–1674.